SEPT6 drives hepatocellular carcinoma cell proliferation, migration and invasion via the Hippo/YAP signaling pathway

YUHUI FAN[1], ZHIPENG DU[2], QIANG DING[2], JIANG ZHANG[1], MARK OP DEN WINKEL[1], ALEXANDER L. GERBES[1], MEI LIU[2] and CHRISTIAN J. STEIB[1]

[1]Department of Medicine II, Liver Center Munich, University Hospital, Ludwig-Maximilians-University of Munich, Munich 81377, Germany; [2]Department of Gastroenterology, Institute of Liver and Gastrointestinal Diseases, Tongji Hospital, Tongji Medical College, Huazhong University of Science and Technology, Wuhan, Hubei 430030, P.R. China

Received October 8, 2020; Accepted March 8, 2021

DOI: 10.3892/ijo.2021.5205

Abstract. Septin 6 (SEPT6) is a member of the GTP-binding protein family that is highly conserved in eukaryotes and regulates various biological functions, including filament dynamics, cytokinesis and cell migration. However, the functional importance of SEPT6 in hepatocellular carcinoma (HCC) is not completely understood. The present study aimed to investigate the expression levels and roles of SEPT6 in HCC, as well as the underlying mechanisms. The reverse transcription quantitative PCR, western blotting and immunohistochemistry staining results demonstrated that SEPT6 expression was significantly elevated in HCC tissues compared with corresponding adjacent non-tumor tissues, which indicated that SEPT6 expression may serve as a marker of poor prognosis for HCC. By performing plasmid transfection and G418 treatment, stable SEPT6-knockdown and SEPT6-overexpression cell lines were established. The Cell Counting Kit-8, flow cytometry and Transwell assay results demonstrated that SEPT6 overexpression significantly increased HCC cell proliferation, cell cycle transition, migration and invasion compared with the Vector group, whereas SEPT6 knockdown displayed significant suppressive effects on HCC cell lines *in vitro* compared with the control group. Mechanistically, SEPT6 might facilitate F-actin formation, which induced large tumor suppressor kinase 1 dephosphorylation, inhibited Hippo signaling, upregulated yes-associated protein (YAP) expression and nuclear translocation, and upregulated cyclin D1 and matrix metallopeptidase 2 (MMP2) expression. Furthermore, YAP overexpression significantly reversed SEPT6 knockdown-induced inhibitory effects on HCC, whereas YAP knockdown significantly inhibited the oncogenic effect of SEPT6 overexpression on HCC. Collectively, the present study demonstrated that SEPT6 may promote HCC progression by enhancing YAP activation, suggesting that targeting SEPT6 may serve as a novel therapeutic strategy for HCC.

Correspondence to: Dr Christian J. Steib, Department of Medicine II, Liver Center Munich, University Hospital, Ludwig-Maximilians-University of Munich, 15 Marchioninistrasse, Munich 81377, Germany
E-mail: fyhmed@yeah.net; christian.steib@med.uni-muenchen.de

Dr Mei Liu, Department of Gastroenterology, Institute of Liver and Gastrointestinal Diseases, Tongji Hospital, Tongji Medical College, Huazhong University of Science and Technology, 1095 Jiefang Avenue, Qiaokou, Wuhan, Hubei 430030, P.R. China
E-mail: tjliumei@yeah.net

Key words: hepatocellular carcinoma, septin 6, proliferation, migration, invasion, Hippo/yes-associated protein signaling pathway

Introduction

In 2018, hepatocellular carcinoma (HCC) was estimated to be the sixth most common cancer and the third most common cause of cancer-related mortality, resulting in ~841,000 new cases and 781,000 deaths worldwide (1,2). Although advances in therapeutic strategies have benefited patients who are diagnosed at an early stage, the majority of patients with HCC are diagnosed at an advanced stage and their overall survival remains poor, which is primarily attributed to the recurrence and metastasis of the disease (3). Therefore, identifying novel causative genes and molecular mechanisms underlying HCC progression is important for the development of therapeutic targets with improved efficacy.

Recent studies revealed that the Hippo signaling pathway is implicated in tumorigenesis and may display tumor suppressor effects (4-6). The core of Hippo signaling consists of macrophage stimulating 1/2, which regulates activation of large tumor suppressor kinase 1/2 (LATS1/2). Active LATS1/2 phosphorylates the downstream transcriptional co-activator Yes-associated protein (YAP)/tafazzin (TAZ). In the cytoplasm, the proteasome mediates ubiquitination and degradation of phosphorylated YAP/TAZ, which suppresses the transcription of proliferation- and survival-associated genes (7). Increasing evidence has indicated that the Hippo signaling pathway is crucial for HCC initiation and progression (8-10). Several factors have been reported to regulate Hippo signaling, including actin cytoskeleton, cell polarity and cell contact (11). Moreover, recent studies have demonstrated that cytoskeletal proteins regulate HCC progression by activating the Hippo signaling pathway (6,12,13).

Septins are highly conserved GTP-binding proteins family incorporating 13 members, which are ubiquitously expressed in the majority of eukaryotes (14). Recently, septins were categorized as the fourth cytoskeletal component, which interacts with cellular membranes, actin filaments and microtubules, and regulates various cellular processes (15). Among the 13 members, septin 6 (SEPT6) primarily regulates filament dynamics, cytokinesis, proliferation, cell cycle transition, survival and chemotaxis (14,16-18). In prostate cancer tissues, SEPT6 expression was decreased, and SEPT6 knockdown contributed to prostate cancer survival and invasion (18). Recently, it was reported that SEPT6 expression was upregulated in liver fibrosis, which promoted hepatic stellate cell activation, proliferation and migration (19). A previous study demonstrated that Hepatitis B surface antigen (HBsAg) knockdown blocked HCC growth, whereas HBsAg knockdown decreased SEPT6 expression in HepG2.2.15 cells (20), indicating that SEPT6 may be involved in HCC pathogenesis. However, the functional importance of SEPT6 in HCC development and the regulation of the Hippo signaling pathway is not completely understood.

The present study aimed to investigate whether SEPT6 expression was upregulated in HCC tissues and to determine its association with prognosis. The effects of SEPT6 overexpression on HCC cell proliferation, cell cycle transition, migration and invasion, and the role of the Hippo signaling pathway and YAP activation were investigated. The results of the present study may indicate a novel therapeutic strategy for HCC.

Materials and methods

HCC samples and cell lines. A total of 64 patients (51 male patients and 13 female patients; age range, 26-78 years; average age, 52.58±12.73) were enrolled in the present study at Tongji Hospital (Wuhan, China) between January 2011 and December 2014. The inclusion criteria were as follows: i) Patients were pathologically diagnosed with HCC; ii) patients underwent surgical excision; and iii) patients were aged >18 years. The exclusion criteria were as follows: i) Patients received preoperative therapy; and ii) patients with more than one primary tumor. The tumor and corresponding adjacent non-tumor (distance from tumor margin, >2 cm) tissues were collected. Tissues were fixed with 4% paraformaldehyde at room temperature for 48 h, embedded in paraffin and sectioned to 5-μm thick sections for immunohistochemistry staining. Alternatively, tissues were immediately preserved at -80˚C for RNA and protein extraction. The clinicopathological characteristics of the patients were recorded, including sex, age, hepatitis B virus infection, α-fetoprotein levels, tumor size, tumor number and metastasis (Table I). Written informed consent was obtained from all patients. The present study was approved by the Ethics Committee of Tongji Hospital (approval no. TJ-IRB20180404) and was conducted according to the principles outlined in the Declaration of Helsinki. Two normal hepatocyte cell lines (THLE-2 and THLE-3), Hep3B and Huh7 were purchased from American Type Culture Collection. MHCC-97L and MHCC-97H were purchased from The Cell Bank of Type Culture Collection of The Chinese Academy of Sciences. HCC-LM3 was obtained from the Liver Cancer Institute, Zhongshan Hospital, Fudan University (Shanghai, China). Cells were cultured in DMEM supplemented with 10% FBS (Gibco; Thermo Fisher Scientific, Inc.), 100 U/ml penicillin and 100 μg/ml streptomycin at 37˚C with 5% CO_2.

Reagent. The F-actin inhibitor latrunculin B (Lat. B) was purchased from Abcam (cat. no. ab144291) and was used following the standard protocol. Briefly, latrunculin B (1 mg) was dissolved in 40 μl DMSO to make a 25 mg/ml stock solution. The stock solution was stored at -20˚C until subsequent use. Before use, Lat. B was thawed and added to DMEM to a final concentration of 10 μM. Cells were treated with Lat. B for 2 h at 37˚C.

Reverse transcription-quantitative PCR (RT-qPCR). Total RNA extraction, reverse transcription, and RT-qPCR were performed following a standard protocol, as previously described (19). Total RNA was extracted from liver tissues and cell lines using TRIzol® reagent (Invitrogen; Thermo Fisher Scientific, Inc.). RNA concentrations were determined using a NanoDrop 2000 Spectrophotometer (Thermo Fisher Scientific, Inc.). Total RNA was reverse transcribed into cDNA using the PrimeScript reagent kit (Takara Biotechnology Co., Ltd.) according to the manufacturer's protocol. The following temperature protocol was used for reverse transcription: 37˚C for 15 min and 85˚C for 5 sec. Subsequently, qPCR was performed using SYBR Premix ExTaq (Takara Biotechnology Co., Ltd.) and an ABI StepOne Real-Time PCR System (Applied Biosystems; Thermo Fisher Scientific, Inc.) according to the manufacturer's protocol. The following thermocycling conditions were used for qPCR: Pre-denaturation at 95˚C for 30 sec; followed by 40 cycles of 95˚C for 5 sec and 60˚C for 30 sec. mRNA expression levels were quantified using the $2^{-\Delta\Delta Cq}$ method (21) and normalized to the internal reference gene β-actin. The sequences of the primers used for qPCR are presented in Table SI.

Western blotting and co-immunoprecipitation (co-IP). Total protein was extracted from liver tissues and cell lines using RIPA buffer containing protease inhibitors PMSF and cocktail (Servicebio Technology Co., Ltd.). Nuclear proteins were extracted using NE-PER (Thermo Fisher Scientific, Inc.). Protein concentrations were determined using a BCA kit (Boster Biological Technology). Western blotting was performed as previously described (19). Briefly, proteins (30 μg per lane) were separated via 10% SDS-PAGE and transferred onto PVDF membranes (EMD Millipore), which were then blocked with 5% BSA (cat. no. 4240GR100; Guangzhou Saiguo Biotech Co., Ltd.) at room temperature for 1 h. Subsequently, the membranes were incubated with primary antibodies at 4˚C overnight. After washing three times in TBST, the membranes were incubated with HRP-conjugated secondary antibodies (Beyotime Institute of Biotechnology) at room temperature for 1 h. After washing three times, protein bands were detected using an ECL assay kit (Advansta, Inc.). Protein expression was semi-quantified using ImageJ software (version 1.44p; National Institutes of Health) with β-actin as the loading control. The primary and secondary antibodies used for western blotting are listed in Table SII.

Table I. Association between SEPT6 expression and clinicopathological variables in human HCC tissues.

Variable	SEPT6 expression		P-value
	Low (n=18)	High (n=46)	
Sex			0.530
Female	4	9	
Male	14	37	
Age (years)			0.578
≤45	6	16	
>45	12	30	
HBsAg			0.291
Negative	5	18	
Positive	13	28	
AFP (ng/ml)			0.172
≤400	8	13	
>400	10	33	
Tumor diameter (cm)			0.010[a]
≤5	11	12	
>5	7	34	
Tumor number			0.490
Single	13	35	
Multiple	5	11	
Metastasis			0.016[a]
No	11	13	
Yes	7	33	

SEPT6 expression was assessed via reverse transcription-quantitative PCR. SEPT6 high/low expression indicated that SEPT6 expression in was higher/lower in HCC tissues compared with corresponding adjacent non-tumor tissues. [a]P<0.05. SEPT6, septin 6; HCC, hepatocellular carcinoma; HBsAg, hepatitis B surface antigen; AFP, α-fetoprotein.

For the co-IP assay, MHCC-97H cells (2-5x10^7) were washed twice with cold PBS twice and lysed using 1% NP-40 buffer (cat. no. P0013F; Beyotime Institute of Biotechnology) containing protease inhibitors at 4˚C for 30 min. After centrifugation at 12,000 x g for 15 min at 4˚C, the supernatant was collected. Protein A/G PLUS-Agarose beads (cat. no. sc-2003; Santa Cruz Biotechnology, Inc.) were washed three times with PBS and diluted in PBS to 50% concentration. Subsequently, the Agarose beads (100 μl/ml) were added to the supernatant (containing 200-600 μg protein). The mixture was incubated for 30 min at 4˚C on a horizontal shaker. After centrifugation at 1,000 x g for 5 min at 4˚C, the supernatant was collected and divided into two parts. SEPT6 antibody (2 μg/500 μg cell lysate) or isotype normal IgG antibody (2 μg/500 μg cell lysate; cat. no. sc-2026; Santa Cruz Biotechnology, Inc.) was added to the supernatant (~500 μl total volume) and incubated for 1 h at 4˚C. Subsequently, additional Agarose beads (100 μl/ml) were added and incubated at 4˚C overnight. After centrifugation at 1,000 x g for 5 min at 4˚C, the supernatant was discarded and the pellets were washed four times with 1.0 ml NP-40 buffer. The samples were boiled with sample loading buffer for 10 min, and the Agarose beads were discarded. The supernatant was collected and analyzed via western blotting using antibodies targeted against SEPT6, LATS1 and LATS2 according to the aforementioned protocol. The antibodies used for co-IP are listed in Table SII.

Immunohistochemistry (IHC) staining. The expression of SEPT6 in HCC samples and corresponding adjacent non-tumor tissues were analyzed by IHC, as previously described (19). Briefly, paraffin-embedded slides were de-paraffinized in xylene and rehydrated using an alcohol gradient. Antigen retrieval was performed by heating samples in 0.01 mol/l citrate buffer (pH 6.0) for 15 min in a microwave. Subsequently, the slides were immersed in 3% H_2O_2 at room temperature for 15 min to eliminate the endogenous peroxidase. After washing three times with PBS, the sections were blocked using 10% goat serum (Boster Biological Technology) at room temperature for 30 min. Subsequently, the sections were incubated with an anti-SEPT6 (cat. no. 12805-1-AP; 1:100; ProteinTech Group, Inc.) at 4˚C overnight. After washing three times with PBS, the sections were incubated with a biotinylated secondary antibody (cat. no. SP-9000; OriGene Technologies, Inc.) at 37˚C for 1 h. After washing three times with PBS, peroxidase activity was visualized using DAB (OriGene Technologies, Inc.) at room temperature for ~10 sec. Then, the sections were counterstained with hematoxylin (OriGene Technologies, Inc.) at room temperature for ~1 min. Stained samples were visualized using an IX71 light microscope (Olympus Corporation; magnification, x100).

Immunofluorescence staining. Huh7 cells (5x10^4 each well) were seeded onto glass cover slides in 24-well plates overnight. Subsequently, cells were fixed with 4% formaldehyde at room temperature for 20 min, permeabilized using 0.3% Triton X-100 and blocked with 5% BSA (cat. no. 4240GR100; BioFroxx; Saiguo Biological Technology Co., Ltd.) at room temperature for 30 min. Subsequently, the slides were incubated with ActinRed (cat. no. KGMP0012; Nanjing KeyGen Biotech Co., Ltd.) at room temperature for 20 min. The nuclei were counterstained with DAPI solution (cat. no. G1012; Wuhan Servicebio Technology Co., Ltd.) at room temperature for 10 min. Stained cells were observed using an IX71 fluorescence microscope (Olympus Corporation; magnification, x400).

Plasmid transfection and stable cell line selection. The plasmids used for SEPT6 and YAP knockdown and overexpression were purchased from Shanghai GeneChem Co., Ltd. At 80-90% confluence, cells were transfected with 2 μg plasmid using Lipofectamine® 3000 (Invitrogen; Thermo Fisher Scientific, Inc.) in Opti-MEM (Gibco; Thermo Fisher Scientific, Inc.) according to the manufacturer's protocol. At 6-8 h post-transfection, the cell culture medium was replaced with DMEM supplemented with 10% FBS. The control shRNA was a non-targeting shRNA and the overexpression control was an empty vector. The shRNA sequences are presented in Table SI. At 48 h post-transfection, transfected cell lines were treated with G418 (400 μg/ml) for 2 weeks to select stably transfected cells. Transfection efficiencies were assessed and the stable cell lines were used for subsequent experiments. The following cell lines were established: MHCC-97H-shcontrol,

MHCC-97H-shSEPT6, Huh7-Vector, Huh7-SEPT6, MHCC-97H-shSEPT6+YAP, Huh7-SEPT6+shYAP, HCC-LM3-shcontrol, HCC-LM3-shSEPT6, Hep3B-Vector and Hep-3B-SEPT6.

Cell Counting Kit-8 (CCK-8) assay. Cell proliferation was detected using the CCK-8 kit (cat. no. C0037; Beyotime Institute of Biotechnology) according to the manufacturer's protocol, as previously described (19). Briefly, cells were seeded ($1x10^3$ cells/well) into 96-well plates and cultured for 24, 48, 72 or 96 h. Subsequently, the culture medium was replaced with 100 μl DMEM and 10 μl CCK-8. After incubation for 2 h, the absorbance of each well was measured at a wavelength of 450 nm using an ELISA reader.

Flow cytometry analysis of the cell cycle. Cell cycle distribution was assessed by flow cytometry, as previously described (22). Briefly, cells ($1x10^6$) were harvested, washed with cold PBS and fixed using 75% ethanol overnight at 4˚C. After washing twice with PBS, cells were incubated with PI staining solution containing RNase (cat. no. KGA511-KGA512; Nanjing KeyGen Biotech Co., Ltd.) at 37˚C for 30 min in the dark. Subsequently, cell cycle distribution was analyzed using a BD FACSVerse flow cytometer (BD Biosciences) and CELLQuestPro software (version 5.1; BD Biosciences).

Transwell assays. Transwell insert chambers (pore size, 8 μm; Corning, Inc.) were used to examine cell invasion and migration, respectively. For the invasion assay, the upper chamber inserts were precoated with Matrigel (BD Biosciences) at 37˚C for 1 h. Briefly, 200 μl serum-free DMEM containing cells ($2x10^4$) was plated into the upper chamber and the lower chamber was filled with 600 μl DMEM supplemented with 20% FBS. Following incubation at 37˚C for 24 h, migratory/invading cells were fixed using absolute methanol at room temperature for 10 min, and stained using 0.2% crystal violet solution at room temperature for 1 h. Cells were observed using an IX71 microscope (Olympus Corporation; magnification, x100) in at least three fields of view.

Database. The Gene Expression Profiling Interactive Analysis (GEPIA) database (gepia.cancer-pku.cn) was used to determine SEPT6 mRNA expression levels in human liver HCC specimens and corresponding adjacent non-tumor specimens.

Statistical analysis. Each experiment was performed in triplicate. Data are presented as the mean ± SD. Statistical analyses were performed using GraphPad Prism (version 5.0; GraphPad Software, Inc.) or SPSS (version 19.0; IBM Corp.) software. Comparisons between two groups were analyzed using the paired or unpaired Student's t-test. Comparisons among multiple groups were analyzed using one-way ANOVA followed by Tukey's post hoc test. Categorical data were analyzed using Fisher's exact test. Patient survival was analyzed via Kaplan-Meier analysis and log-rank tests. $P<0.05$ was considered to indicate a statistically significant difference.

Results

SEPT6 is upregulated in human HCC and predicts poor prognosis. To examine SEPT6 expression in HCC, SEPT6 mRNA expression levels were assessed in 64 paired HCC samples. Compared with corresponding adjacent non-tumor samples, SEPT6 mRNA expression levels were significantly higher in 46 paired HCC samples (71.88%; Fig. 1A). Subsequently, we selected 20 paired tissues, including 16 paired tissues with higher SEPT6 mRNA expression in the HCC tisues compared with the adjacent non-tumor tissues, and 4 paired tissues with lower SEPT6 mRNA expression in HCC tissues compared with the adjacent non-tumor tissues. The protein expression levels of SEPT6 were determined via western blotting. The results demonstrated that the protein expression levels of SEPT6 were significantly higher in 16 HCC tissues compared with the adjacent non-tumor tissues (Fig. 1B and S1A, C and D), whereas the protein expression levels of SEPT6 were significantly lower in 4 HCC tissues compared with the adjacent non-tumor tissues (Fig. S1B), indicating a positive association between mRNA and protein expression levels of SEPT6 in human patients with HCC. The association between SEPT6 expression levels and clinicopathological characteristics was investigated. SEPT6 expression levels were significantly associated with tumor size and metastasis, but not significantly associated with sex, age, hepatitis B virus infection, tumor number or α-fetoprotein levels (Table I). Furthermore, the association between SEPT6 expression and overall survival was assessed. SEPT6 high/low expression represented that SEPT6 expression in the HCC tissues was higher/lower compared with the corresponding adjacent non-tumor tissues (fold change >1.5), respectively. The results demonstrated that high SEPT6 expression levels indicated significantly worse overall survival in patients with HCC compared with low SEPT6 expression levels (Fig. 1C). IHC staining demonstrated that SEPT6 expression levels were notably higher in HCC samples compared with corresponding adjacent non-tumor samples, and SEPT6 protein expression was primarily localized in the cytoplasm (Fig. 1D). In addition, analysis of the GEPIA database demonstrated significantly upregulated SEPT6 expression in HCC compared with adjacent non-tumor tissues (Fig. 1E). Subsequently, SEPT6 expression levels were examined in two normal hepatocyte cell lines (THLE-2 and THLE-3) and several HCC cell lines. Among HCC cell lines, MHCC-97H and HCC-LM3 cells display the highest metastatic potential (23-25). The results suggested that SEPT6 expression was significantly higher in the majority of the HCC cell lines, particularly in those with high metastatic potential (MHCC-97H and HCC-LM3), compared with normal hepatocytes (Fig. 1F and G). Collectively, the results indicated that SEPT6 expression was upregulated in human HCC and may serve as a predictor of poor prognosis.

SEPT6 promotes HCC cell proliferation. Subsequently, gain- and loss-of-function assays were performed to assess the effect of SEPT6 on HCC cell function. Following assessment of SEPT6 endogenous expression levels in different HCC cells, MHCC-97H and Huh7 cells were selected for SEPT6 knockdown or overexpression, respectively, and stably transfected cells were established. Transfection efficiencies were determined by measuring SEPT6 mRNA and protein expression levels (Fig. 2A and C). The CCK-8 assay results indicated that SEPT6 knockdown significantly inhibited MHCC-97H cell proliferation compared with the control group, whereas SEPT6

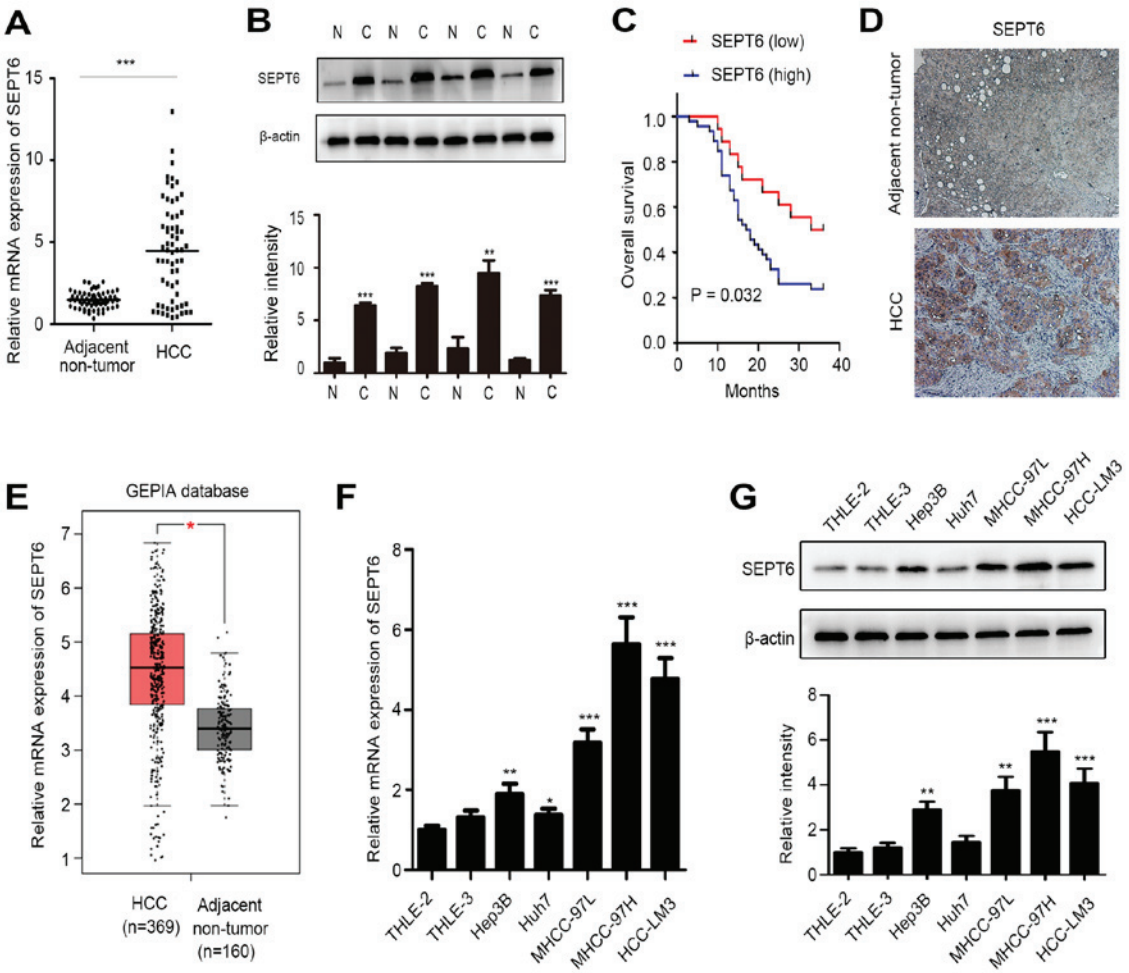

Figure 1. SEPT6 is upregulated in human HCC and predicts poor prognosis. (A) SEPT6 mRNA expression levels in 64 paired HCC samples and adjacent non-tumor tissues were assessed via RT-qPCR. (B) SEPT6 protein expression levels in HCC samples (n=4) and corresponding adjacent non-tumor samples (n=4) were assessed via western blotting. (C) Association between SEPT6 expression and overall survival as determined by Kaplan-Meier survival analysis. SEPT6 low expression (n=18) and SEPT6 high expression (n=46). (D) SEPT6 staining in HCC samples and corresponding adjacent non-tumor samples (magnification, x100). (E) SEPT6 expression in HCC and corresponding adjacent non-tumor samples derived from the GEPIA database. SEPT6 (F) mRNA and (G) protein expression levels in the normal hepatocyte cell lines and HCC cell lines were determined via RT-qPCR and western blotting, respectively. *P<0.05, **P<0.01 and ***P<0.001 vs. N or THLE2. SEPT6, septin 6; HCC, hepatocellular carcinoma; RT-qPCR, reverse transcription-quantitative PCR; GEPIA, Gene Expression Profiling Interactive Analysis; N, adjacent non-tumor tissues; C, HCC tissues.

overexpression significantly increased Huh7 cell proliferation compared with the Vector group (Fig. 2B). Subsequently, flow cytometry was performed to investigate whether SEPT6 regulated the cell cycle. Compared with the control group, SEPT6 knockdown resulted in significantly increased cell cycle arrest at the G_1/S phase in MHCC-97H cells, but displayed no significant effect on the G_2/M transition (Fig. 2D). By contrast, compared with the Vector group, SEPT6 overexpression significantly promoted G_1/S transition in Huh7 cells, but had no significant effect on G_2/M transition. The results suggested that SEPT6 primarily regulated the G_1/S transition, whereas its effect on the G_2/M transition was not significant. Furthermore, cyclin D1 and cyclin E1 expression levels are significantly associated with G_1/S cell cycle transition (15). The RT-qPCR results indicated that SEPT6 knockdown significantly decreased cyclin D1 expression in MHCC-97H cells compared with the control group, whereas SEPT6 overexpression significantly increased cyclin D1 expression in Huh7 cells compared with the Vector group (Fig. 2E). However, cyclin E1 mRNA expression levels were not significantly altered by SEPT6 knockdown or overexpression compared with the control and Vector groups, respectively. Consistent results were obtained for protein expression levels (Fig. 2F). Collectively, the results indicated that SEPT6 promoted HCC cell proliferation and G_1/S transition *in vitro*.

SEPT6 promotes HCC cell migration and invasion. Metastasis is the leading cause of HCC-related mortality (26). The Transwell assay results demonstrated that SEPT6 knockdown significantly decreased MHCC-97H cell migration and invasion compared with the control group, whereas SEPT6 overexpression significantly increased Huh7 cell migration and invasion compared with the Vector group (Fig. 3A and B). Moreover, matrix metallopeptidase (MMP)2 expression levels were significantly decreased by SEPT6 knockdown in MHCC-97H cells compared with the control group, whereas SEPT6 overexpression significantly increased MMP2 expression levels in Huh7 cells compared with the Vector group (Fig. 3C). However, MMP9 mRNA expression levels were not significantly altered in response to SEPT6 knockdown or overexpression compared

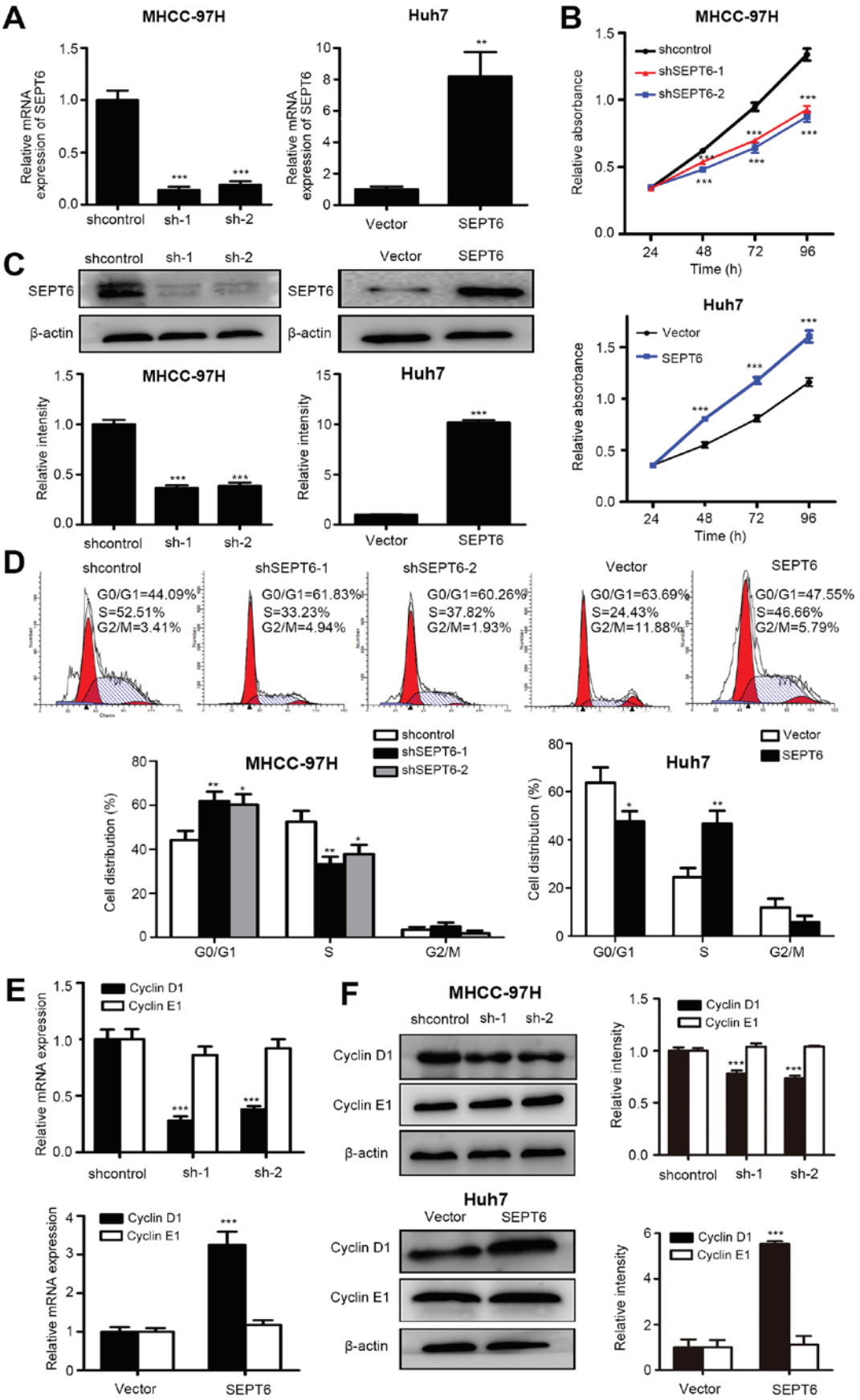

Figure 2. SEPT6 promotes HCC cell proliferation. SEPT6-knockdown MHCC-97H and SEPT6-overexpression Huh7 cells were established by transfection with the corresponding plasmids. At 48 h post-transfection, cells were treated with G418 (400 μg/ml) for 2 weeks for stable cell selection. (A) Transfection efficiencies were determined via RT-qPCR. (B) Cell Counting Kit-8 assays were performed to assess cell proliferation. (C) Transfection efficiencies were also determined via western blotting. (D) Flow cytometry was conducted to analyze cell cycle distribution. Cyclin D1 and cyclin E1 (E) mRNA and (F) protein expression levels were measured via RT-qPCR and western blotting, respectively. *P<0.05, **P<0.01 and ***P<0.001 vs. shcontrol or Vector. SEPT6, septin 6; HCC, hepatocellular carcinoma; RT-qPCR, reverse transcription-quantitative PCR; sh, short hairpin RNA.

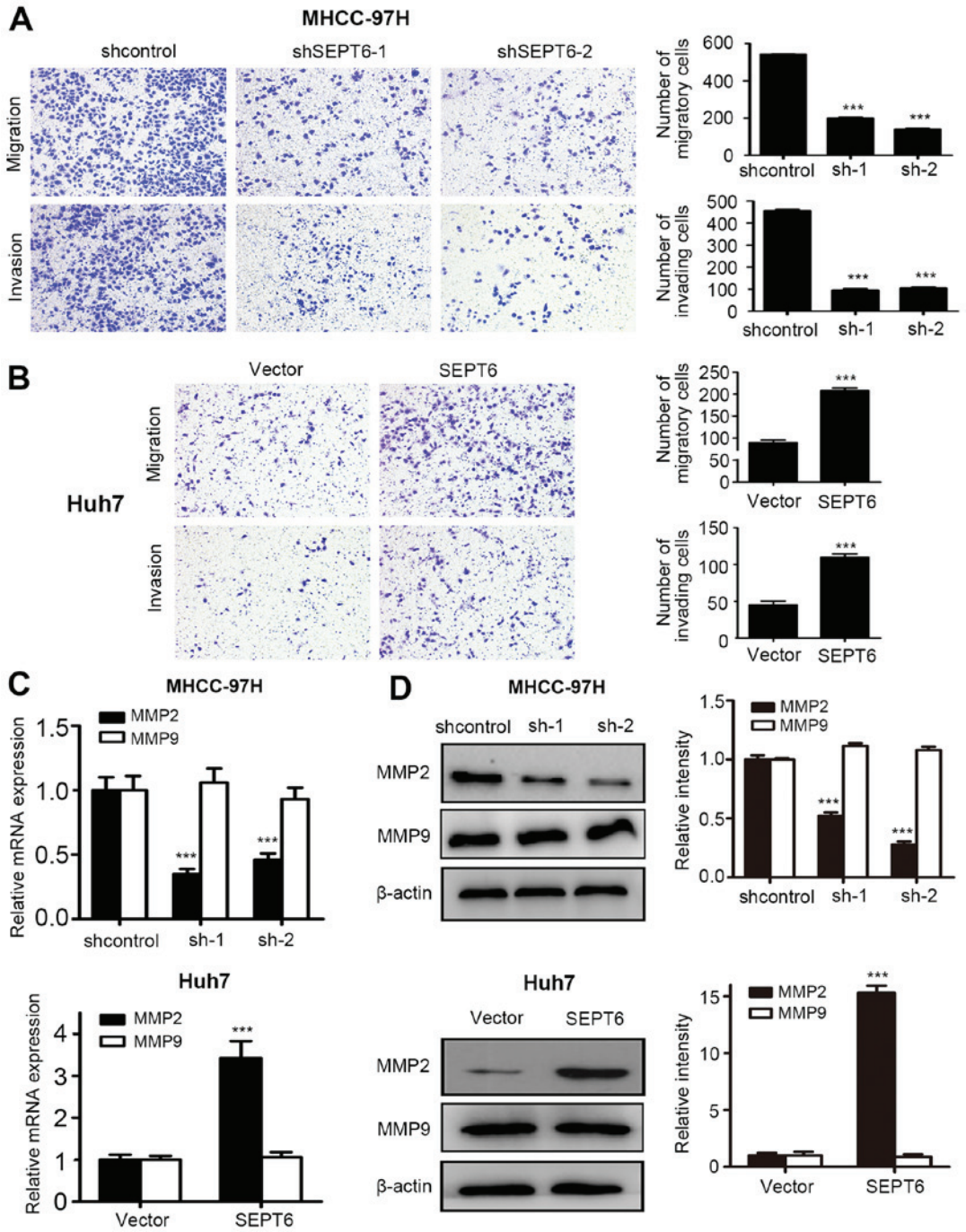

Figure 3. SEPT6 promotes HCC cell migration and invasion. Transwell assays were conducted to assess (A) MHCC-97H and (B) Huh7 cell migration and invasion (magnification, x100). MMP2 and MMP9 (C) mRNA and (D) protein expression levels were measured via reverse transcription-quantitative PCR and western blotting, respectively. ***P<0.001 vs. shcontrol or Vector. SEPT6, septin 6; HCC, hepatocellular carcinoma; MMP, matrix metallopeptidase; sh, short hairpin RNA.

with the control and Vector groups, respectively (Fig. 3C). Similar results were obtained via western blotting (Fig. 3D). Collectively, the *in vitro* results demonstrated that SEPT6 enhanced HCC cell migration and invasion.

SEPT6 regulates the Hippo/YAP signaling pathway in HCC. As aforementioned, SEPT6 promoted HCC cell proliferation and migration; therefore, the mechanism underlying its action was investigated. Increasing evidence has demonstrated that Hippo signaling is crucial for HCC tumorigenesis and metastasis (8-10). Furthermore, Hippo signaling is primarily regulated by the actin cytoskeleton (11). Septin proteins are considered as the fourth cytoskeletal component and SEPT6 regulates actin cytoskeleton dynamics (15); therefore, the present study further investigated whether SEPT6 promoted HCC cell progression by regulating Hippo signaling. The transfection efficiency of SEPT6 knockdown and overexpression in HCC-LM3 and Hep3B cells, respectively, was verified via RT-qPCR and western blotting (Fig. S2). The western blotting results indicated that compared with the control group, SEPT6 knockdown significantly promoted the phosphorylation of LATS1 and YAP in MHCC-97H and HCC-LM3 cells, but notably decreased the overall expression of YAP. By contrast, compared with the vector group, SEPT6

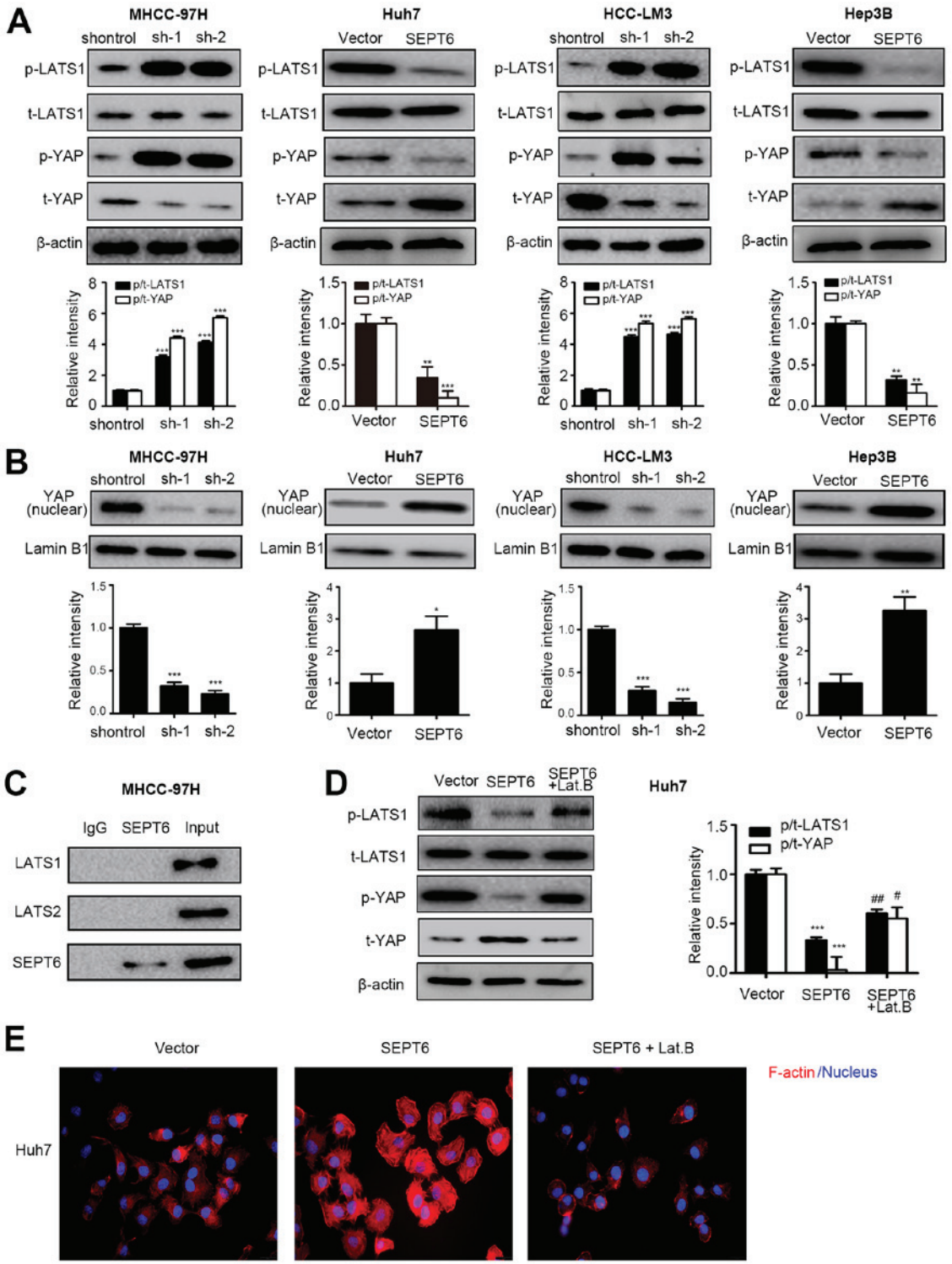

Figure 4. SEPT6 regulates the Hippo/YAP signaling pathway in HCC. (A) p-LATS1, LATS1, p-YAP and YAP protein expression levels were measured via western blotting. (B) Nuclear YAP protein expression levels were measured via western blotting using Lamin B1 as the loading control. (C) Co-immunoprecipitation assays were performed to determine the interaction between SEPT6 and LATS1 or LATS2. SEPT6-overexpression Huh7 cells were treated with 10 μM Lat. B for 2 h to disrupt the cytoskeleton. (D) Protein expression levels of p-LATS1, LATS1, p-YAP and YAP were measured via western blotting. (E) F-actin formation was determined by performing immunofluorescence assays (magnification, x400). *P<0.05, **P<0.01 and ***P<0.001 vs. shcontrol or Vector; $^{\#}$P<0.05 and $^{\#\#}$P<0.01 vs. SEPT6. SEPT6, septin 6; YAP, yes-associated protein; HCC, hepatocellular carcinoma; p, phosphorylated; LATS1, large tumor suppressor kinase 1; Lat. B, Latrunculin B; t, total; sh, short hairpin RNA.

overexpression significantly decreased the phosphorylation of LATS1 and YAP, and markedly increased the overall expression of YAP both in Huh7 and Hep3B cells (Fig. 4A). The results indicated that SEPT6 may regulate the activity of Hippo signaling, while modulating the activity, stability and overall expression of YAP. Subsequently, the present study examined whether SEPT6 regulated YAP nuclear translocation. The western blotting results demonstrated that SEPT6 knockdown significantly decreased nuclear YAP protein expression levels in MHCC-97H and HCC-LM3 cells compared with the

control group, whereas SEPT6 overexpression significantly upregulated nuclear YAP protein expression levels in Huh7 and Hep3B cells compared with the Vector group (Fig. 4B). The results suggested that SEPT6 upregulation may inactivate Hippo signaling by inhibiting the phosphorylation of LATS1, which resulted in inhibition of YAP phosphorylation, as well as proteasome-induced YAP ubiquitination and degradation. Therefore, higher protein expression levels of YAP were translocated to the nucleus, resulting in enhanced gene transcription.

Furthermore, an endogenous co-IP assay was performed to investigate whether SEPT6 interacted with LATS1 and LATS2. The results indicated that SEPT6 did not directly interact with LATS (Fig. 4C). Septins, the fourth component of the cytoskeleton, lack the kinase activity domain (6); therefore, SEPT6 may regulate LATS1 phosphorylation indirectly, which may be associated with the cytoskeleton-regulating function of the septin proteins. To verify this hypothesis, SEPT6-overexpression Huh7 cells were treated with the F-actin inhibitor Lat. B to disrupt the cytoskeleton. Subsequently, F-actin levels and the phosphorylated and overall expression levels of LATS1 and YAP were assessed. The results indicated that compared with the vector group, SEPT6 overexpression notably facilitated F-actin formation, which was markedly disrupted by Lat. B (Fig. 4E). Furthermore, Lat. B treatment increased LATS1 and YAP phosphorylation, thus notably decreasing YAP overall expression in SEPT6-overexpression Huh7 cells (Fig. 4D). Collectively, the results indicated that SEPT6 may regulate Hippo/YAP signaling in HCC by modulating F-actin formation.

SEPT6 regulates HCC cell proliferation, cell cycle progression, migration and invasion via the Hippo/YAP signaling pathway. The present study further investigated whether SEPT6 exerted its effects via regulating the Hippo/YAP signaling pathway. Firstly, the transfection efficiencies of YAP-overexpression plasmids in MHCC-97H cells and YAP-knockdown plasmids in Huh7 cells were verified by measuring mRNA and protein expression levels, which suggested that these plasmids were appropriate for YAP overexpression and knockdown (Fig. S3). Subsequently, YAP was overexpressed by plasmid transfection in stable SEPT6-knockdown MHCC-97H cells and stable cells were selected by G418. YAP upregulation in MHCC-97H-shSEPT6 cells was validated by protein expression analysis (Fig. 5A). Compared with the control group, SEPT6 knockdown significantly decreased MHCC-97H cell proliferation, G_1/S transition, migration and invasion (Fig. 5B-D). SEPT6 knockdown-induced effects were significantly reversed by YAP overexpression. YAP downregulation was achieved by shRNA transfection in stable SEPT6-overexpression Huh7 cells, and stable cells were selected for further experiments. YAP knockdown was verified in Huh7-SEPT6 cells (Fig. 5E). Compared with the Vector group, SEPT6 overexpression significantly enhanced Huh7 cell proliferation, migration, invasion and G_1/S phase transition (Fig. 5F-H). SEPT6 overexpression-mediated effects were significantly reversed by YAP knockdown. Furthermore, the present study assessed whether YAP was involved in SEPT6-regulated cyclin D1 and MMP2 expression. YAP overexpression significantly upregulated cyclin D1 and MMP2 expression levels in SEPT6-knockdown MHCC-97H cells, whereas YAP knockdown significantly decreased cyclin D1 and MMP2 expression levels in SEPT6-overexpression Huh7 cells (Fig. 5I). Furthermore, to analyze SEPT6-independent effects of YAP on the regulation of cyclin D1 and MMP2 expression, four stable cell lines were established by plasmid transfection and G418 selection using Huh7 cells, namely Huh7-Vector, Huh7-SEPT6, Huh7-shYAP and Huh7-shYAP-SEPT6. Compared with the Vector group, SEPT6 overexpression significantly upregulated cyclin D1 and MMP2 expression levels, whereas YAP knockdown not only inhibited SEPT6-mediated effects on cyclin D1 and MMP2 expression, but also significantly decreased cyclin D1 and MMP2 expression levels (Fig. S4). Collectively, the results demonstrated that the Hippo/YAP signaling axis may serve a key role in SEPT6-induced HCC cell proliferation, cell cycle progression, migration and invasion.

Discussion

HCC is the third leading cause of cancer-related mortality, and its prognosis is extremely poor due to early relapse and metastasis following curative resection (3). Although various therapeutic targets have been identified, the prognosis of patients with HCC remains poor (3). To the best of our knowledge, the present study was the first to demonstrate that SEPT6 inhibited Hippo signaling, activated the downstream effector YAP, and enhanced cyclin D1 and MMP2 expression levels, which promoted HCC growth and metastasis.

SEPT6 is primarily implicated in hematological malignancies (27), nervous system development (16) and tumor progression (18). In prostate cancer, SEPT6 expression is downregulated, and SEPT6 knockdown promotes cancer cell survival and invasion, suggesting a tumor suppressor role (18). However, the present study demonstrated that SEPT6 expression was significantly increased in HCC tissues compared with corresponding adjacent non-tumor tissues, which was associated with poor prognosis. The results prompted investigation into why SEPT6 expression was upregulated in HCC tissues. It was hypothesized that the malignant transformation of tumor cells and the complicated tumor microenvironment, which involves hypoxia, inflammatory cytokines stimulation, metabolic reprogramming and epigenetic regulation, might be the leading causes for SEPT6 upregulation in HCC. Moreover, the leading cause of HCC and whether the causes work synergistically requires further investigation. SEPT6 overexpression significantly enhanced HCC cell proliferation, cell cycle transition, migration and invasion compared with the Vector group, whereas SEPT6 knockdown displayed the opposite effects compared with the control group. Therefore, SEPT6 was identified as an oncogene in HCC, which contrasted to its role in prostate cancer. It was previously reported that SEPT6 promoted liver fibrogenesis (19). Since liver fibrosis and liver cirrhosis are considered as the precancerous states of HCC, it is reasonable to hypothesize that SEPT6 may promote HCC progression. The results of the present study indicated that the expression patterns and effects of SEPT6 in prostate cancer and HCC were opposite, which may be due to different genetic backgrounds, including gene mutation, or the tumor microenvironment. The roles of certain proteins are context-dependent; therefore, the difference in the tumor

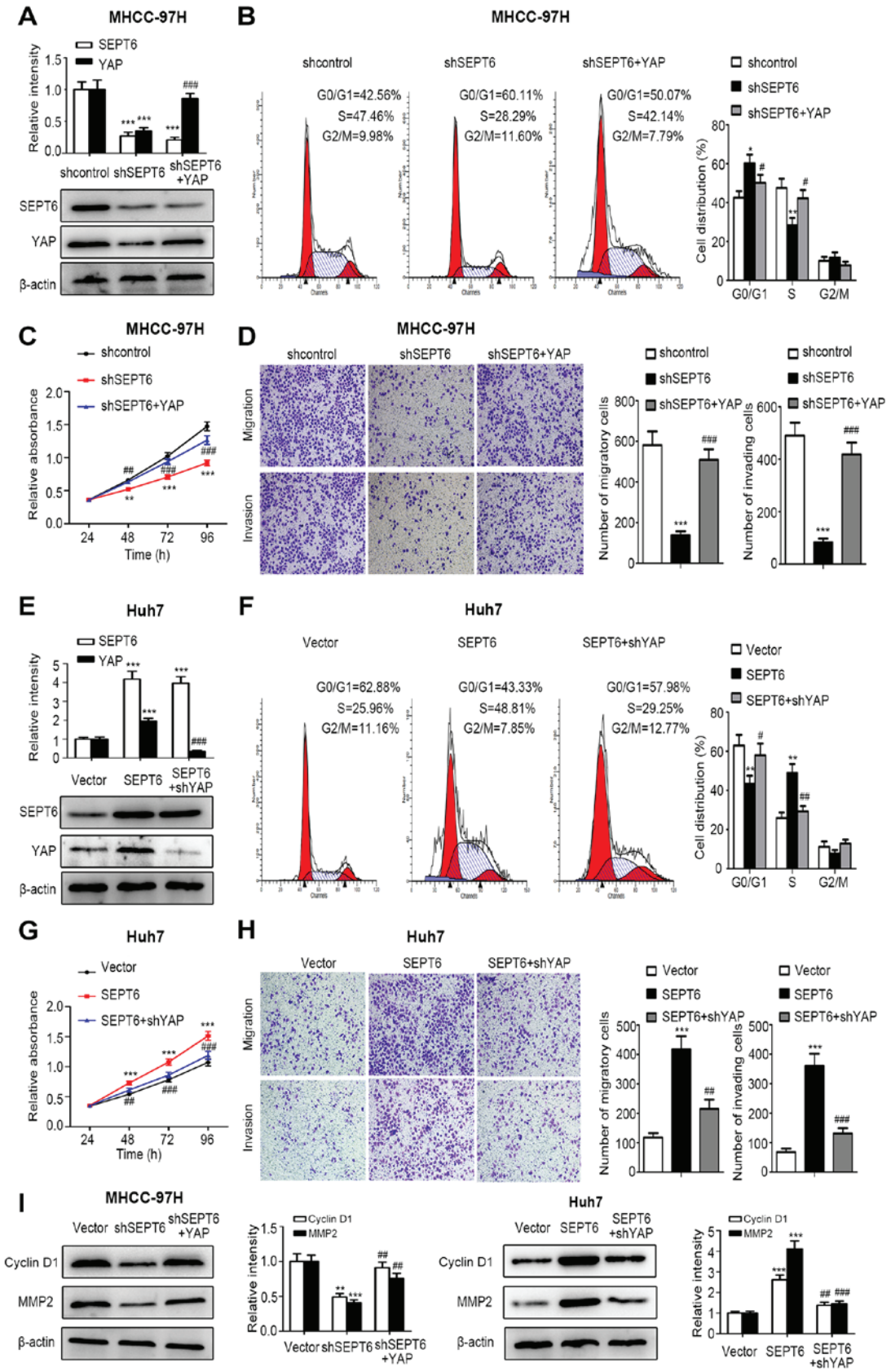

Figure 5. SEPT6 regulates HCC cell proliferation, cell cycle progression, migration and invasion via the Hippo/YAP signaling pathway. MHCC-97H-shSEPT6 cells were transfected with YAP and stable Huh7-SEPT6 cells were transfected with shYAP. Subsequently, G418 was used for stable cell selection. (A) Transfection efficiencies of shSEPT6 and YAP were determined via western blotting. MHCC-97H cell (B) cycle distribution, (C) proliferation, (D) migration and invasion (magnification, x100) were assessed by performing CCK-8, flow cytometry and Transwell assays, respectively. (E) Transfection efficiencies of SEPT6 and shYAP were determined via western blotting. Huh7 cell (F) cycle distribution, (G) proliferation, (H) migration and invasion (magnification, x100) were assessed by performing CCK-8, flow cytometry and Transwell assays, respectively. (I) Cyclin D1 and MMP2 protein expression levels were determined via western blotting. *P<0.05, **P<0.01 and ***P<0.001 vs. Vector; $^{\#}$P<0.05, $^{\#\#}$P<0.01 and $^{\#\#\#}$P<0.001 vs. shSEPT6 or SEPT6. SEPT6, septin 6; HCC, hepatocellular carcinoma; YAP, yes-associated protein; sh, short hairpin RNA; CCK-8, Cell Counting Kit-8; MMP2, matrix metallopeptidase 2.

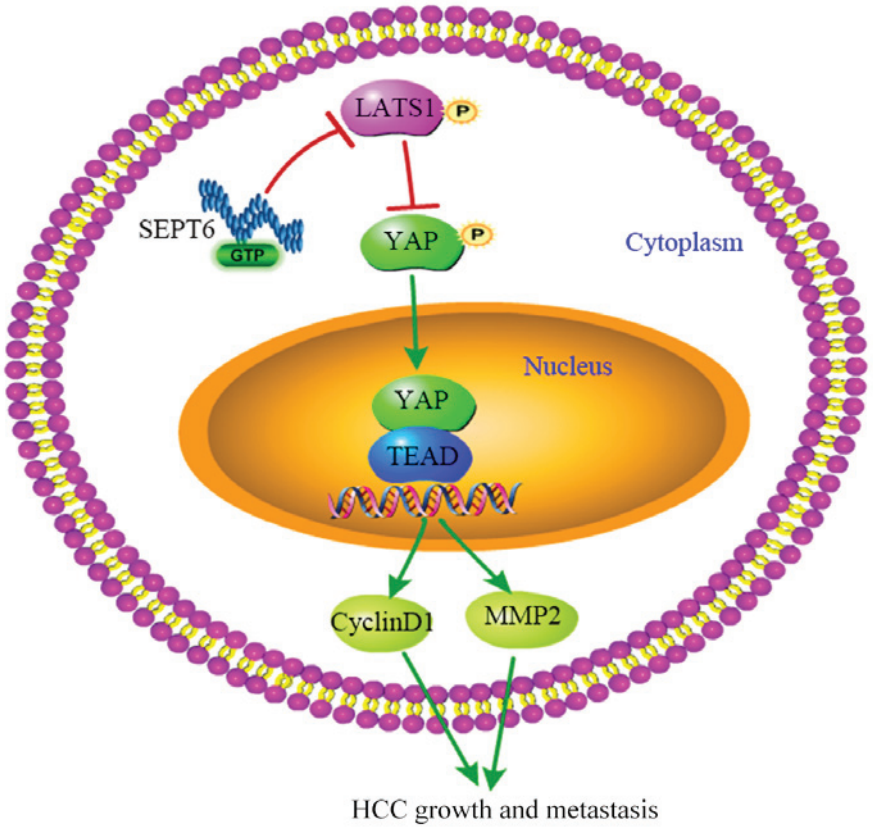

Figure 6. Summary of SEPT6-regulated Hippo/YAP signaling pathway in HCC. SEPT6 expression was upregulated in HCC, which inactivated Hippo signaling, dephosphorylated and stabilized the downstream effector YAP and upregulated YAP expression. Subsequently, active YAP was translocated to the nucleus and promoted transactivation of cyclin D1 and MMP2, resulting in HCC cell proliferation and metastasis. SEPT6, septin 6; YAP, yes-associated protein; HCC, hepatocellular carcinoma; MMP2, matrix metallopeptidase 2; TEAD, TEA domain transcription factor; p, phosphorylated

microenvironment between HCC and prostate cancer may result in different expression patterns and functional roles of SEPT6.

Subsequently, the mechanism underlying the oncogenic action of SEPT6 was examined. The present study focused on the Hippo signaling pathway, which is crucial for HCC tumorigenesis and progression (8-10). Hippo signaling is primarily regulated by the actin cytoskeleton (11). For example, the cytoskeletal protein PDZ and LIM domain 1 inhibited HCC metastasis by activating Hippo signaling (6). SEPT6 has been reported to regulate actin and microtubule remodeling (17). Based on the aforementioned studies, the potential role of SEPT6 in promoting HCC progression in a Hippo/YAP-dependent manner was assessed. The results indicated that compared with the Vector group, SEPT6 overexpression inactivated Hippo signaling, and dephosphorylated and stabilized the downstream effector YAP, leading to the translocation of active YAP into the nucleus and the transactivation of cyclin D1 and MMP2, which resulted in HCC cell proliferation and metastasis (Fig. 6). Furthermore, YAP knockdown significantly reversed the oncogenic effects of SEPT6 overexpression on HCC progression, whereas YAP overexpression significantly reversed SEPT6 knockdown-mediated inhibitory effects. As previously reported, YAP regulates cyclin D1 and MMP2 expression independently, regardless of SEPT6 expression (26,28-30). The results of the present study also demonstrated that YAP knockdown inhibited SEPT6-mediated upregulation of cyclin D1 and MMP2 expression. The results demonstrated that SEPT6 regulated cyclin D1 and MMP2 expression via YAP, and YAP independently regulated cyclin D1 and MMP2 expression to a certain extent.

The regulatory mechanism underlying Hippo signaling has received increasing attention. Hippo signaling can be regulated by mechanical force, the extracellular matrix, cell-cell contact and cytoskeletal interactions (7,11,31,32). With regard to cytoskeletal interactions, Hippo signaling can be regulated by F-actin levels, F-actin activity and cytoskeletal tension (11). In HCC cell lines, F-actin was confirmed to bind to LATS1, resulting in the dephosphorylation and inactivation of Hippo signaling (6). Furthermore, the Rho GTPase serves an important role in regulating Hippo signaling activity by the cytoskeleton (31). Septins belong to a family of GTP-binding proteins and are considered as the fourth cytoskeletal component. In addition, SEPT6 was reported to regulate actin cytoskeleton dynamics (14,15). Based on previous studies, it was hypothesized that SEPT6 may regulate Hippo via three possible mechanisms, one of which involves the regulation of F-actin formation by SEPT6 in order to affect cytoskeleton dynamics. Subsequently, F-actin binds to LATS1 and causes Hippo inactivation. The hypothesis was confirmed by the present study, since compared with the Vector group, SEPT6 overexpression notably facilitated F-actin formation, whereas disruption of F-actin by Lat. B abrogated SEPT6-induced LATS1 dephosphorylation and Hippo inactivation. Furthermore, whether SEPT6 regulates other proteins associated with cytoskeleton dynamics, including Ezrin and neurofibromin 2 (NF2), requires further investigation. Previous

studies reported that Ezrin and NF2 were involved in the regulation of Hippo signaling (33,34). Secondly, as a GTP-binding protein, SEPT6 may regulate GTPase activity and thus, Hippo signaling activity. Finally, it may be possible that SEPT6 mediates the recruitment of certain phosphatases to repress LATS1 phosphorylation. Collectively, the results of the present study indicated a possible mechanism by which SEPT6 regulated Hippo signaling via upregulation of F-actin formation. However, further investigation of the underlying mechanism is required.

In conclusion, the present study demonstrated that SEPT6 was upregulated in HCC and displayed an oncogenic function in HCC progression. SEPT6 promoted HCC cell proliferation, cell cycle progression, migration and invasion, which was mediated at least partly via the SEPT6/Hippo/YAP axis. Therefore, the results of the present study may provide novel insight into HCC treatment.

Acknowledgements

Not applicable.

Funding

The present study was supported by the Deutsche Forschungsgemeinschaft (grant nos. DFG STE 1022/2-3 and DFG STE 1022/4-1), the National Natural Science Foundation of China (grant nos. 81272657 and 81572422) and the China Scholarship Council (grant nos. 201908080017 and 201606230249).

Availability of data and materials

The datasets used and/or analyzed during the present study are available from the corresponding author upon reasonable request.

Authors' contributions

YF performed the cytologic and mechanistic experiments. ZD and QD analyzed the data. JZ analyzed the clinical data. QD and JZ confirm the authenticity of all the raw data. MODW and ALG made substantial contributions to the conception of the study and drafted the manuscript. ML and CJS designed the study and revised the manuscript. All authors read and approved the final manuscript.

Ethics approval and consent to participate

The present study was approved by the Tongji Hospital Ethics Committee (approval no. TJ-IRB20180404). Written informed consent was obtained from each patient in accordance with the ethical standards of the World Medical Association Declaration of Helsinki.

Patient consent for publication

Not applicable.

Competing interests

The authors declare that they have no competing interests.

References

1. Yang JD, Hainaut P, Gores GJ, Amadou A, Plymoth A and Roberts LR: A global view of hepatocellular carcinoma: Trends, risk, prevention and management. Nat Rev Gastroenterol Hepatol 16: 589-604, 2019.
2. Bray F, Ferlay J, Soerjomataram I, Siegel RL, Torre LA and Jemal A: Global cancer statistics 2018: GLOBOCAN estimates of incidence and mortality worldwide for 36 cancers in 185 countries. CA Cancer J Clin 68: 394-424, 2018.
3. Kanwal F and Singal AG: Surveillance for hepatocellular carcinoma: Current best practice and future direction. Gastroenterology 157: 54-64, 2019.
4. Ji S, Liu Q, Zhang S, Chen Q, Wang C, Zhang W, Xiao C, Li Y, Nian C, Li J, *et al*: FGF15 activates Hippo signaling to suppress bile acid metabolism and liver tumorigenesis. Dev Cell 48: 460-474.e9, 2019.
5. Dent P, Booth L, Roberts JL, Liu J, Poklepovic A, Lalani AS, Tuveson D, Martinez J and Hancock JF: Neratinib inhibits Hippo/YAP signaling, reduces mutant K-RAS expression, and kills pancreatic and blood cancer cells. Oncogene 38: 5890-5904, 2019.
6. Huang Z, Zhou JK, Wang K, Chen H, Qin S, Liu J, Luo M, Chen Y, Jiang J, Zhou L, *et al*: PDLIM1 inhibits tumor metastasis through activating Hippo signaling in hepatocellular carcinoma. Hepatology 71: 1643-1659, 2020.
7. Meng Z, Moroishi T and Guan KL: Mechanisms of Hippo pathway regulation. Genes Dev 30: 1-17, 2016.
8. Zhou D, Conrad C, Xia F, Park JS, Payer B, Yin Y, Lauwers GY, Thasler W, Lee JT, Avruch J, *et al*: Mst1 and Mst2 maintain hepatocyte quiescence and suppress hepatocellular carcinoma development through inactivation of the Yap1 oncogene. Cancer Cell 16: 425-438, 2009.
9. Feng X, Lu T, Li J, Yang R, Hu L, Ye Y, Mao F, He L, Xu J, Wang Z, *et al*: The tumor suppressor interferon regulatory factor 2 binding protein 2 regulates Hippo pathway in liver cancer by a feedback loop in mice. Hepatology 71: 1988-2004, 2020.
10. Li Y, Lu J, Chen Q, Han S, Shao H, Chen P, Jin Q, Yang M, Shangguan F, Fei M, *et al*: Artemisinin suppresses hepatocellular carcinoma cell growth, migration and invasion by targeting cellular bioenergetics and Hippo-YAP signaling. Arch Toxicol 93: 3367-3383, 2019.
11. Sun S and Irvine KD: Cellular organization and cytoskeletal regulation of the Hippo signaling network. Trends Cell Biol 26: 694-704, 2016.
12. Chen Q, Zhou XW, Zhang AJ and He K: ACTN1 supports tumor growth by inhibiting Hippo signaling in hepatocellular carcinoma. J Exp Clin Cancer Res 40: 23, 2021.
13. Yang XM, Cao XY, He P, Li J, Feng MX, Zhang YL, Zhang XL, Wang YH, Yang Q, Zhu L, *et al*: Overexpression of Rac GTPase activating protein 1 contributes to proliferation of cancer cells by reducing Hippo signaling to promote cytokinesis. Gastroenterology 155: 1233-1249.e22, 2018.
14. Longtine MS, DeMarini DJ, Valencik ML, Al-Awar OS, Fares H, De Virgilio C and Pringle JR: The septins: Roles in cytokinesis and other processes. Curr Opin Cell Biol 8: 106-119, 1996.
15. Mostowy S and Cossart P: Septins: The fourth component of the cytoskeleton. Nat Rev Mol Cell Biol 13: 183-194, 2012.
16. Hu J, Bai X, Bowen JR, Dolat L, Korobova F, Yu W, Baas PW, Svitkina T, Gallo G and Spiliotis ET: Septin-driven coordination of actin and microtubule remodeling regulates the collateral branching of axons. Curr Biol 22: 1109-1115, 2012.
17. Kremer BE, Adang LA and Macara IG: Septins regulate actin organization and cell-cycle arrest through nuclear accumulation of NCK mediated by SOCS7. Cell 130: 837-850, 2007.
18. Wei Y, Yang J, Yi L, Wang Y, Dong Z, Liu Z, Ou-yang S, Wu H, Zhong Z, Yin Z, *et al*: MiR-223-3p targeting SEPT6 promotes the biological behavior of prostate cancer. Sci Rep 4: 7546, 2014.
19. Fan Y, Du Z, Steib CJ, Ding Q, Lu P, Tian D and Liu M: Effect of SEPT6 on the biological behavior of hepatic stellate cells and liver fibrosis in rats and its mechanism. Lab Invest 99: 17-36, 2019.
20. Xiangji L, Feng X, Qingbao C, Weifeng T, Xiaoqing J, Baihe Z, Feng S, Hongyang W and Mengchao W: Knockdown of HBV surface antigen gene expression by a lentiviral microRNA-based system inhibits HBV replication and HCC growth. J Viral Hepat 18: 653-660, 2011.
21. Livak KJ and Schmittgen TD: Analysis of relative gene expression data using real-time quantitative PCR and the 2(-Delta Delta C(T)) method. Methods 25: 402-408, 2001.

22. Kondo R, Ishino K, Wada R, Takata H, Peng WX, Kudo M, Kure S, Kaneya Y, Taniai N, Yoshida H, *et al*: Downregulation of protein disulfide isomerase A3 expression inhibits cell proliferation and induces apoptosis through STAT3 signaling in hepatocellular carcinoma. Int J Oncol 54: 1409-1421, 2019.
23. Li Y, Tang ZY and Hou JX: Hepatocellular carcinoma: Insight from animal models. Nat Rev Gastroenterol Hepatol 9: 32-43, 2011.
24. Sun F, Wang J, Sun Q, Li F, Gao H, Xu L, Zhang J, Sun X, Tian Y, Zhao Q, *et al*: Interleukin-8 promotes integrin β3 upregulation and cell invasion through PI3K/Akt pathway in hepatocellular carcinoma. J Exp Clin Cancer Res 38: 449, 2019.
25. Ding ZB, Shi YH, Zhou J, Shi GM, Ke AW, Qiu SJ, Wang XY, Dai Z, Xu Y and Fan J: Liver-intestine cadherin predicts microvascular invasion and poor prognosis of hepatitis B virus-positive hepatocellular carcinoma. Cancer 115: 4753-4765, 2009.
26. Xia H, Dai X, Yu H, Zhou S, Fan Z, Wei G, Tang Q, Gong Q and Bi F: EGFR-PI3K-PDK1 pathway regulates YAP signaling in hepatocellular carcinoma: The mechanism and its implications in targeted therapy. Cell Death Dis 9: 269, 2018.
27. Cerveira N, Bizarro S and Teixeira MR: MLL-SEPTIN gene fusions in hematological malignancies. Biol Chem 392: 713-724, 2011.
28. Pan Y, Tong JH, Lung RW, Kang W, Kwan JS, Chak WP, Tin KY, Chung LY, Wu F, Ng SS, *et al*: RASAL2 promotes tumor progression through LATS2/YAP1 axis of hippo signaling pathway in colorectal cancer. Mol Cancer 17: 102, 2018.
29. Zhang J, Xu ZP, Yang YC, Zhu JS, Zhou Z and Chen WX: Expression of Yes-associated protein in gastric adenocarcinoma and inhibitory effects of its knockdown on gastric cancer cell proliferation and metastasis. Int J Immunopathol Pharmacol 25: 583-590, 2012.
30. Xie K, Xu C, Zhang M, Wang M, Min L, Qian C, Wang Q, Ni Z, Mou S, Dai H, *et al*: Yes-associated protein regulates podocyte cell cycle re-entry and dedifferentiation in adriamycin-induced nephropathy. Cell Death Dis 10: 915, 2019.
31. Zhang C, Wang F, Gao Z, Zhang P, Gao J and Wu X: Regulation of Hippo signaling by mechanical signals and the cytoskeleton. DNA Cell Biol 39: 159-166, 2020.
32. Matsui Y and Lai ZC: Mutual regulation between Hippo signaling and actin cytoskeleton. Protein Cell 4: 904-910, 2013.
33. Xue Y, Bhushan B, Mars WM, Bowen W, Tao J, Orr A, Stoops J, Yu Y, Luo J, Duncan AW, *et al*: Phosphorylated Ezrin (Thr567) regulates Hippo pathway and yes-associated protein (Yap) in liver. Am J Pathol 190: 1427-1437, 2020.
34. Matsuda T, Zhai P, Sciarretta S, Zhang Y, Jeong JI, Ikeda S, Park J, Hsu CP, Tian B, Pan D, *et al*: NF2 activates Hippo signaling and promotes ischemia/reperfusion injury in the heart. Circ Res 119: 596-606, 2016.